



Adsorption of catechol by Zr-loaded carbon nanotubes from solution

Keke Zhu, Yifan Gu, Rong Wang*, Runping Han*

College of Chemistry, Green Catalysis Center, Zhengzhou University, No. 100 of Kexue Road, Zhengzhou 450001, China, emails: wangjoya@zzu.edu.cn (R. Wang), rphan67@zzu.edu.cn (R. Han), 1791825116@qq.com (K. Zhu), 503153641@qq.com (Y. Gu)

Received 12 July 2021; Accepted 11 August 2021

ABSTRACT

Catechol in water seriously affects the oxygen balance in the water and endangers the human nervous system. Therefore, the removal of phenolic organic compounds from water is of vital importance. Zr-modified carboxylic multi-walled carbon nanotubes (Zr-cCNTs) were prepared by chemical precipitation method and the adsorption properties toward catechol were studied. The maximum adsorption capacity of Zr-cCNTs for catechol was 42.7 mg g^{-1} , which greatly improved the adsorption ability for catechol on carboxylic multi-walled carbon nanotubes (cMWCNTs). The adsorption of catechol onto Zr-cCNTs was slightly affected by pH and the coexistence of Cl^- and SO_4^{2-} in an aqueous solution. The adsorption process of catechol by Zr-cCNTs accorded with Freundlich and Koble–Corrigan models. The adsorption kinetics confirmed to the Elovich and pseudo-second-order kinetic model, which indicated that the adsorption was dominated by chemical adsorption and there was an ion exchange process. The thermodynamic study showed that the adsorption of catechol by Zr-cCNTs was a spontaneous, endothermic and entropy-increasing physical and chemical adsorption process. But after adsorbing catechol, the desorption and regeneration effect of Zr-cCNTs was poor, which also showed that Zr-cCNTs had a strong binding force to catechol. Moreover, the adsorption capacity and adsorption constant of Zr-cCNTs for catechol in single-component and mix-component systems were higher than other adsorbates. This proved that Zr-cCNTs showed selectivity for the adsorption of catechol due to the presence of o-dihydroxyl in the catechol structure. The mechanism is major complexation through X-ray photoelectron spectroscopy analysis and experimental results. The synthesized adsorbent Zr-cCNTs had excellent adsorption capacity and could be used in the adsorption treatment of related wastewater.

Keywords: Zirconium-modified carbon nanotubes; Adsorption; Catechol; Mechanism

1. Introduction

Water is the source of life. However, with the development of industrialization in recent years, the problem of water pollution has become increasingly serious. Phenolic wastewater is a kind of common industrial wastewater, mainly from coking, oil refining, petrochemical, gas power station, pesticide, chemical industry, paper making, synthetic fiber and other industries [1,2]. The high oxygen consumption of phenolic wastewater will break the oxygen balance in the water and endanger the water and aquatic

organisms [3]. Drinking phenol-contaminated water for a long time will cause dizziness, anemia and various neurological disorders [4]. The Environmental Protection Agency requires that the concentration of phenolic compounds in wastewater be less than 1 mg L^{-1} [5]. Therefore, in order to protect the living things in water and human health, it is vital to remove these pollutants from wastewater and meet dischargeable standards.

Researchers have tried various methods to remove phenolic pollutants from the solution. Xie et al. [6] used activated carbon as an adsorbent to remove phenol from

* Corresponding authors.

wastewater, and the results showed that commercial activated carbon was an effective adsorbent to remove phenol from wastewater. Wang et al. [7] studied the reduction of phenolic compounds in wastewater from a coking plant in Gansu by the aldol condensation-ozone oxidation method. The results illustrated that the concentration of phenolic compounds decreased from 764.7 to 22.4 mg L⁻¹ after 2 h of ozonation. In their study, *m*-methylphenol, *p*-methylphenol and *p*-ethylphenol were completely removed. The adsorption method is widely concerned due to its high efficiency, simplicity and wider application scope in the wastewater treatment process [8].

Carbon nanotubes (CNTs), as a new carbon material with abundant nano-pore structure and large specific surface area, can be used as a good adsorbent in the field of water treatment. Researchers found that CNTs or their composites have good adsorption properties for metal ions, dyes, phenols, organic compounds and inorganic anions. Mohammadi and Veisi et al. [9] synthesized glycine- β -cyclodextrin functionalized carbon nanotubes, which were used for adsorption of dye solution. The results suggested that the removal of Methylene blue, Acid blue 113, Methyl orange, and Disperse red 1 were all over 95%, and the maximum adsorption capacity was 90.9, 172, 96.2, and 500 mg g⁻¹, respectively. The adsorbent has good recycling performance. Ruan et al. [10] prepared one novel composite material hydroxyapatite/multi-walled CNTs using a simple in-situ sol-gel method. The adsorption material has a high fluoride adsorption capacity, with a maximum adsorption capacity of 30.2 mg g⁻¹. The adsorption reaction is mainly caused by anion exchange and electrostatic attraction. Kamaraj and Vasudevan [11] prepared MWCNT by refluxing with nitric acid at 120°C for 2 h to remove selenate from an aqueous solution. The adsorption process was studied systematically by changing the pH value, ionic strength and temperature. The results showed that the adsorption capacity can reach 1.865 mg g⁻¹ when the initial concentration of Se(VI) is 2.0 mg L⁻¹ at 303 K. Thus, MWCNT could be considered as an excellent Se(VI) adsorbent with good application prospects.

Zirconium has good chemical stability and can form five-membered rings with *o*-dihydroxy. Liu et al. [12] successfully prepared the supported zirconium-loaded chitosan/Fe₃O₄/GO. At 313 K, the adsorption capacity of alizarin red reached 231 mg g⁻¹, which was highly effective for the removal of alizarin red. Huang et al. [13] coated the outer surface of Fe₃O₄@SiO₂ core with a layer of Zr-MOFs by the in-situ growth method. Three amino derivatives were prepared with different precursor systems with good adsorption properties for organic dyes and metal ions. The results demonstrated that the anionic and cationic dyes can be selectively removed from the mixed solution only by adjusting the pH of the solution. Ma et al. [14] used the adsorbent obtained by loading Zr on PEI@Fe₃O₄ by precipitation method to adsorb phosphate, which greatly expanded the applicable range of pH.

In previous studies, Huang et al. [15] developed a highly cross-linked resin adsorbent HJ-1. This adsorbent is soluble in water and has an adsorption capacity of 30 mg g⁻¹ for catechol with an initial concentration of 100 mg L⁻¹. However, the adsorption process took 5 h to reach equilibrium. Xu et al. [16] prepared g-C₃N₄/Fe₃O₄ composite materials as an adsorbent by the co-precipitation method. When the initial

concentration of catechol was 50 mg L⁻¹, the removal rate of catechol could reach 70% at pH = 6. But when the pH value increased to 9, the removal rate decreased significantly. But there is seldom study about Zr-modified CNTs to remove catechol from solution. In this study, Zr-modified carboxylic multi-walled carbon nanotubes (Zr-cCNTs) were prepared by a chemical precipitation method for the adsorption of catechol. Zr-cCNTs overcame the disadvantage of low adsorption capacity and limitations of applicable pH range and effect of common salts. Furthermore, the mechanism was discussed through the analysis of X-ray photoelectron spectroscopy (XPS).

2. Materials and methods

2.1. Materials

Reagents: carboxylic multi-walled carbon nanotubes (cMWCNTs) with the purity of 95%, an ID of 2–5 nm, an OD of less than 8 nm and a length of 10–30 μ m. Zirconium oxychloride octahydrate, sodium hydroxide, hydrochloric acid, catechol, sodium chloride, sodium sulfate, and ethanol were all analytical grade and the experimental water was distilled water.

2.2. Preparation of Zr-cCNTs

The adsorbent (Zr-cCNTs) was prepared by the chemical precipitation method, referring to the research of Gu et al. [17] in our laboratory. The same mass of cMWCNTs and ZrOCl₂·8H₂O was added into a 500 mL conical flask. Then add 100 mL distilled water, mixing and oscillating evenly. NaOH solution was added to adjust the pH to about 10. The solution oscillated for 10 h at 303 K and the supernatant was discarded after standing for a few minutes. Carbon nanotubes modified by zirconium (Zr-cCNTs) were prepared after centrifugal washing with purified water to neutralize. The schematic of preparation of Zr-cCNTs is shown in Fig. 1.

Comparing the specific surface area of the materials before and after modification, it obviously decreases (from 500 to 250 m² g⁻¹). This may be caused by the zirconium particles deposited on the surface of cMWCNTs blocking some of the pores [18], indicating that the process is not based on physical adsorption. According to the characterization results of Gu [17], the isoelectric point of cMWCNTs was 5.20. The isoelectric point of Zr-cCNTs was 7.20. The increase of the isoelectric point value of Zr-cCNTs was caused by the increase of basic functional groups on the surface of the material, which may due to the deposition of zirconium hydroxide.

The results of transmission electron microscopy and Raman spectroscopy demonstrated that the zirconium was deposited on the surface of cMWCNTs successfully, and the structure of carbon nanotubes was not damaged during the modification process. Results of FTIR suggested that the C=O vibration peak disappeared and the adsorption peak at 3,438 cm⁻¹ was significantly enhanced, which may be caused by the vibration of –OH in bound water and Zr–OH [19]. The absorption peaks at 1,620 and 1,075 cm⁻¹ were mainly due to the bending vibration of –OH in ZrO(OH)₂ [20,21], indicating that zirconium was successfully deposited on the surface of cMWCNTs.

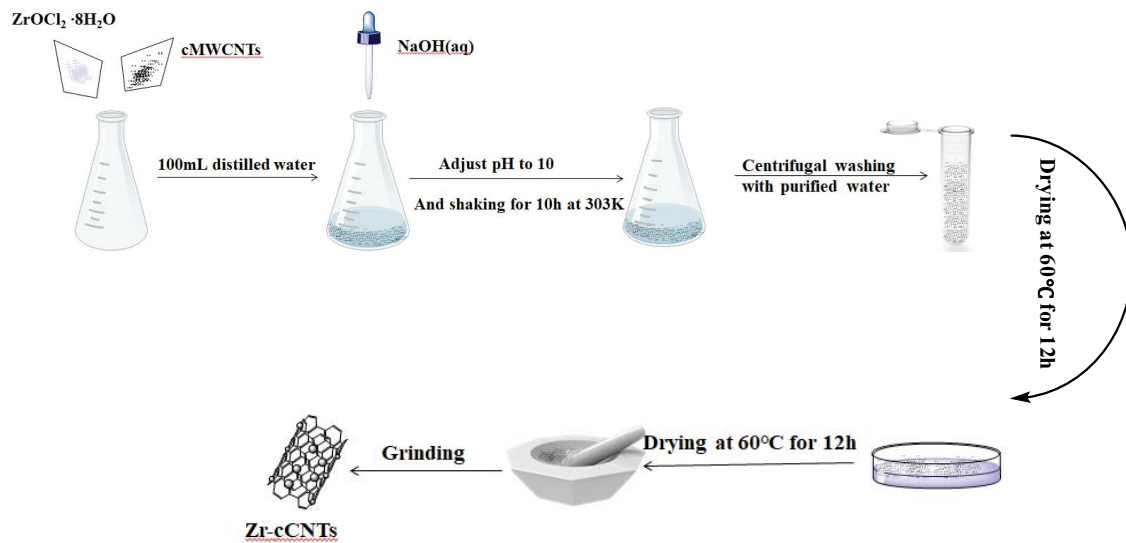


Fig. 1. Schematic of preparation of Zr-cCNTs.

2.3. Adsorption experiments

Adsorption test was performed at 50 mL glass conical flask with 20 mL of the known catechol solution and 0.020 g Zr-cCNTs, with the exception of the study to evaluate the effect of dose on adsorption. Then the flasks were agitated for an amount of time under a constant speed of 120 rpm with a constant temperature. The effects of adsorbent dosage, initial pH of the solution, reaction time, co-existing ions, the equilibrium concentration of solution and temperature on the adsorption process were mainly investigated in the experiment. According to Eqs. (1) and (2), the adsorption quantity q and removal ratio p was calculated, respectively:

$$q = \frac{V(C_0 - C)}{m} \quad (1)$$

$$p = \frac{C_0 - C}{C_0} \times 100\% \quad (2)$$

where q is the unit adsorption capacity (mg g^{-1}) at time t or equilibrium, m is the mass of adsorbent (g), V is the volume (L) of catechol solution, C_0 is the concentration of catechol before adsorption (mg L^{-1}), C is the adsorbed mass concentration after adsorption (mg L^{-1}), p is removal efficiency (%).

2.4. Desorption experiments

In order to recycle the adsorbent, the desorption and regeneration ability of the adsorbent was investigated in batch mode. The adsorption was performed at 303 K with solution pH = 7 and $C_0 = 200 \text{ mg L}^{-1}$, and the unit adsorption capacity of its first adsorption is recorded as q_0 . The various solutions were used to regenerate the spent Zr-cCNTs. Then Zr-cCNTs is again used to adsorb catechol from the solution. The unit adsorption quantity q_n (n is the regeneration times) of the Zr-cCNTs is calculated, m_d is the mass

of desorbed catechol, and m_0 is the remaining catechol mass on the Zr-cCNTs before desorption. The desorption rate d (%) and regeneration rate r (%) of the Zr-cCNTs can be calculated by Eqs. (3) and (4).

$$d = \frac{m_d}{m_0} \times 100\% \quad (3)$$

$$r = \frac{q_n}{q_0} \times 100\% \quad (4)$$

3. Results and discussion

3.1. Adsorption studies

3.1.1. Comparison of the adsorption performance toward catechol

Fig. 2a shows the comparison of the adsorption capacity of cMWCNTs and Zr-cCNTs at different times. It was observed that the equilibrium adsorption capacity of cMWCNTs and Zr-cCNTs to catechol was 9.40 and 33.9 mg g^{-1} , respectively. Obviously, the adsorption capacity of carbon nanotubes to catechol was significantly improved after Zr modification.

3.1.2. Effect of adsorbent dosage on adsorption

The mass of the adsorbent can affect the adsorption quantity. The values of q_e and removal efficiency are depicted in Fig. 1b with an increase of Zr-cCNTs dose. As in Fig. 1b, the removal efficiency of catechol by Zr-cCNTs increased from 7.70% to 59.9% when the mass of Zr-cCNTs increased from 0.002 to 0.020 g, while the unit adsorption capacity decreased from 38.5 to 29.9 mg g^{-1} . This was because, with the increase of adsorbent dosage, the number of active sites gradually increased, so the removal rate increased. However, the concentration of catechol remained unchanged, increasing

the mass of Zr-cCNTs and reducing the amount of the catechol around the unit adsorbent, so the unit adsorption capacity gradually decreased. Considering the unit adsorption capacity and removal rate, 0.010 g was chosen as the dosage of Zr-cCNTs for subsequent experiments.

3.1.3. Effect of pH and salt concentration on adsorption

The solution pH may have an effect on the surface charge of the adsorbent, so the effect of the pH of the solution was explored. The results were shown in Fig. 3a. It can be seen in Fig. 3a, the unit adsorption capacity of Zr-cCNTs toward catechol was about 33.9 mg g^{-1} in the pH range of 2~9, which was slightly affected by the pH value of the solution. This was the same as the results of Gulley-Stahl et al. [22], suggesting that the adsorption of catechol on Zr-cCNTs was mainly due to the formation of inner complexes. Thus, the pH value of the solution was not adjusted in subsequent experiments (pH near 6.0).

The research on the ionic strength of adsorbents is an important aspect of adsorption research because it promotes the practical application of adsorbents [23]. For this study,

two common salts (NaCl and Na_2SO_4) were used and the results were shown in Fig. 3b.

It was clearly seen that with the increase of salt concentration, the adsorption capacity of Zr-cCNTs toward catechol was basically unchanged. In other words, the coexisting ions had no significant effect on the adsorption of catechol by Zr-cCNTs. This indicated that the adsorption of Zr-cCNTs had excellent selectivity for binding catechol. Studies have shown that if Zr-cCNTs and adsorbents form an outer complex, the presence of coexisting ions will have a negative effect on adsorption. However, if an inner complex was formed between Zr-cCNTs and adsorbents, the adsorption was not affected by ionic strength [24]. Similar results were observed by other studies about composites containing Zr toward adsorbates containing o-dihydroxy in one benzene ring [25].

3.1.4. Effect of contact time and kinetic studies

Effect of contact time is often important to be considered. Fig. 4 shows the influence of reaction time on the uptake of catechol onto Zr-cCNTs.

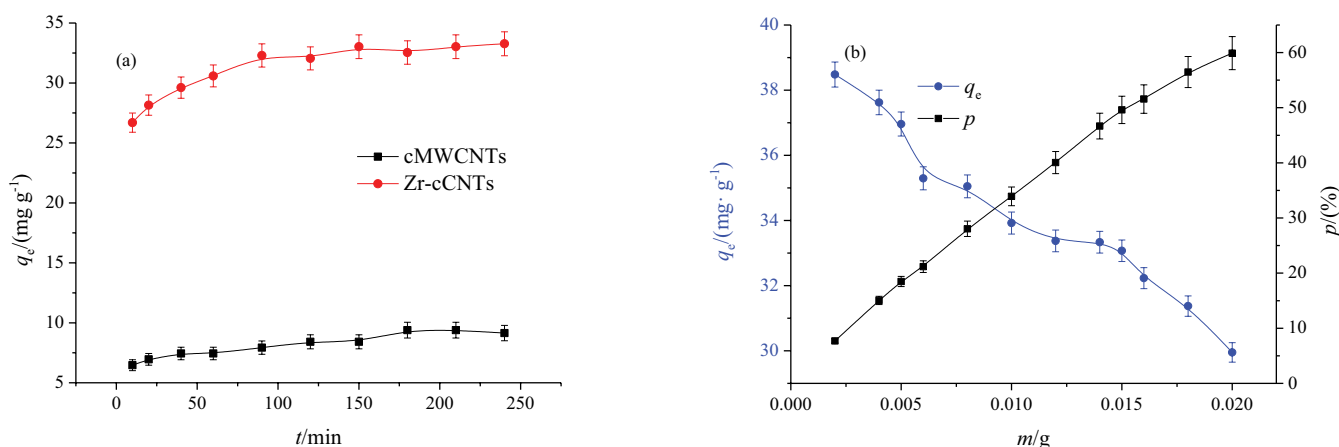


Fig. 2. (a) Comparison of adsorption performance and (b) effect of adsorbent dosage on adsorption.

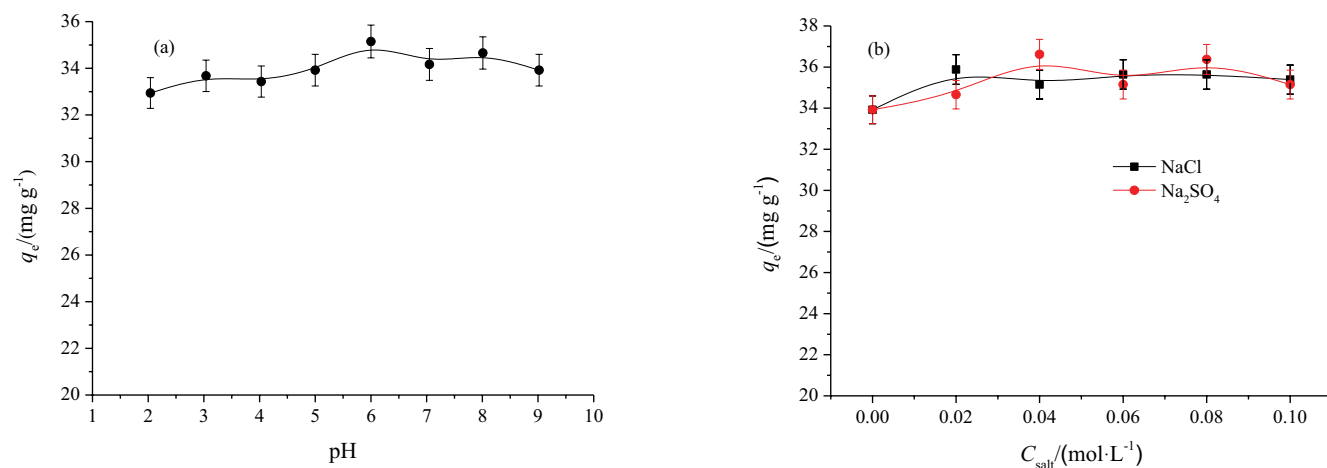


Fig. 3. Effect of pH (a) and co-existing ions (b) on the adsorption of catechol.

It can be seen from Fig. 4 that the adsorption equilibrium time of Zr-cCNTs for catechol was comparatively short. Within 90 min, the adsorption capacity of Zr-cCNTs of catechol enhanced sharply with the increase of reaction time. Subsequently, the growth rate slowed down and tended to equilibrium around 150 min. With the increase of temperature, the adsorption capacity of Zr-cCNTs to catechol is enhanced. This showed that heating was beneficial to the adsorption reaction.

The kinetic models were used to match the experimental data. The correlation coefficient R^2 and error analysis were used to evaluate the fitting degree of the model. Pseudo-second-order and Double Constant models were selected to fit the experimental data. The expressions of the models are as follows.

Pseudo-second-order kinetic model:

$$q_t = \frac{k_2 q_e^2 t}{1 + k_2 q_e t} \quad (5)$$

Double Constant models:

$$\ln q_t = \ln A + k_s t \quad (6)$$

where k_2 and k_s refer to second-order and Double Constant rate coefficient respectively; q_t and q_e are the amounts of Zr-cCNTs adsorbed at time t and at equilibrium (mg g^{-1}), respectively; and A is a constant.

The nonlinear regressive analysis is selected to obtain the parameters of models and the results are listed in Table 1. The fitted curves are also presented in Fig. 4. According to Table 1, in the Double Constant equation, except for the conditions of 293 K and 150 mg L^{-1} , the values of R^2 were greater than 0.900, and SSE is relatively small. Considering the values of R^2 and SSE comprehensively, the results suggested that the adsorption process of catechol by Zr-cCNTs was in accordance with Double Constant models, and was mainly heterogeneous chemical adsorption. The $q_{e(\text{theo})}$ and $q_{e(\text{exp})}$ of the pseudo-second-order model had little difference, indicating that this model can

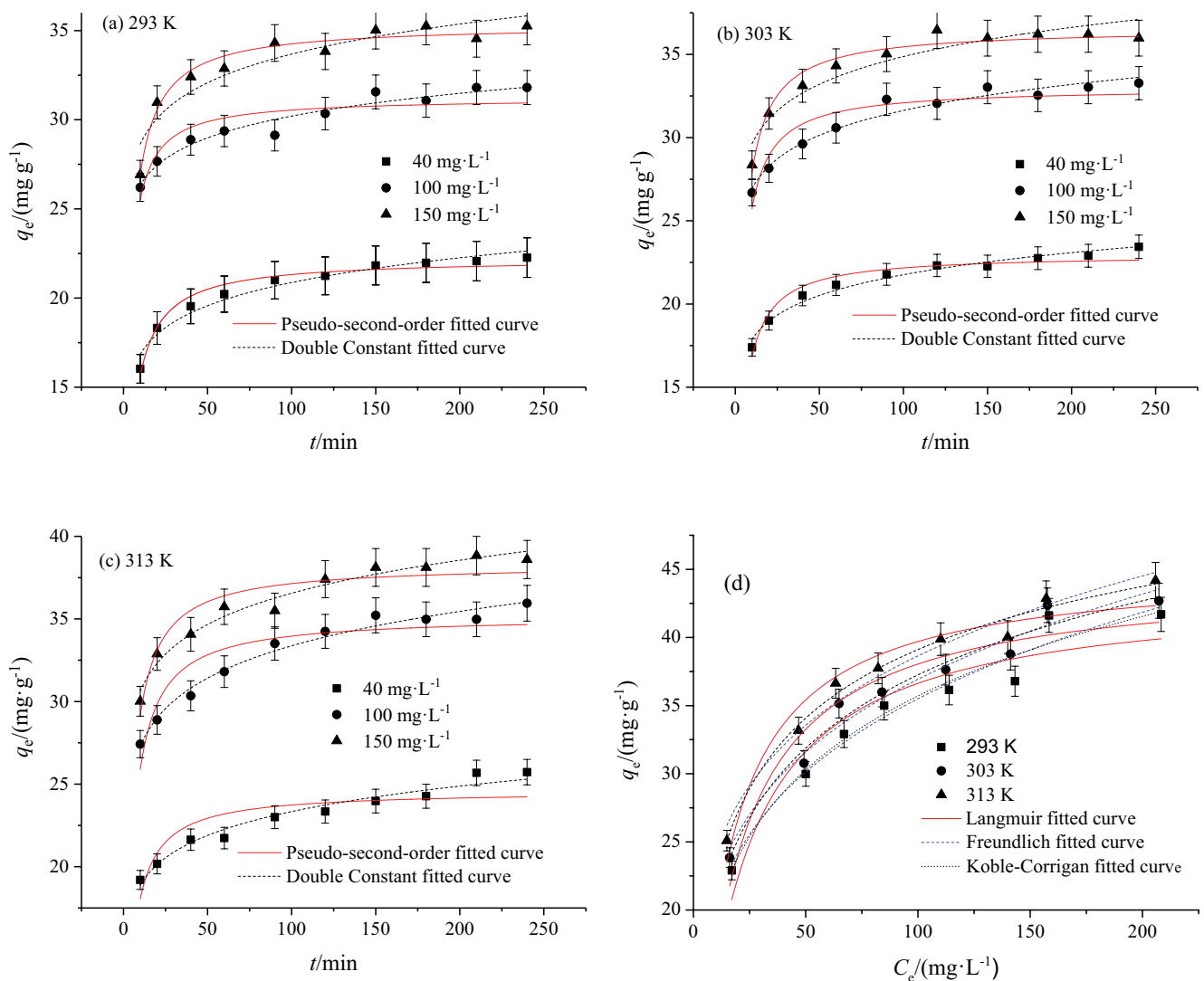


Fig. 4. Kinetic curves (a) 293, (b) 303 K, (c) 313 K and adsorption isotherm curves (d) of catechol adsorption.

Table 1
Kinetic fitting parameters for adsorption of catechol by Zr-cCNTs

Pseudo-second-order equation						
T/K	C_0 /(mg L ⁻¹)	$q_{e(\text{exp})}$ /(mg g ⁻¹)	$q_{e(\text{theo})}$ /(mg g ⁻¹)	k_z /(g mg ⁻¹ min ⁻¹)	R ²	SSE
293	40	22.2	22.2 ± 0.2	0.0107 ± 0.0010	0.961	1.25
	100	31.8	31.2 ± 0.4	0.0143 ± 0.0029	0.796	5.82
	150	35.2	35.3 ± 0.2	0.00907 ± 0.00074	0.965	1.87
303	40	23.4	22.9 ± 0.2	0.0118 ± 0.0014	0.932	1.97
	100	33.2	32.9 ± 0.4	0.0107 ± 0.0016	0.881	4.99
	150	35.9	36.5 ± 0.2	0.00884 ± 0.00073	0.964	2.02
313	40	25.7	24.6 ± 0.5	0.0112 ± 0.0028	0.740	9.94
	100	35.9	35.2 ± 0.6	0.00793 ± 0.0015	0.832	11.8
	150	38.6	38.3 ± 0.5	0.00831 ± 0.0013	0.879	8.04

Double Constant equation					
T/K	C_0 /(mg L ⁻¹)	A	k_s	R ²	SSE
293	40	13.6 ± 0.4	0.0929 ± 0.0069	0.956	1.39
	100	22.9 ± 0.5	0.0596 ± 0.0047	0.948	1.46
	150	24.3 ± 1.0	0.0705 ± 0.0092	0.873	6.80
303	40	14.7 ± 0.3	0.0853 ± 0.0048	0.974	0.740
	100	22.9 ± 0.5	0.0697 ± 0.0046	0.964	1.50
	150	25.2 ± 0.9	0.0707 ± 0.0079	0.903	5.41
313	40	15.3 ± 0.4	0.0921 ± 0.0063	0.962	1.45
	100	22.3 ± 0.4	0.0873 ± 0.0043	0.979	1.41
	150	25.7 ± 0.6	0.0767 ± 0.0485	0.967	2.19

Note: $SSE = \sum (q - q_c)^2$, q and q_c are values from the experiments and calculation according the model, respectively.

be used to predict equilibrium adsorption. However, the R^2 value was ($0.740 \leq R^2 \leq 0.965$) with a large change, and SSE was greater than 1. Furthermore, the fitted curves from the Double Constant equation were closer to experimental points than those from the pseudo-second-order model. Therefore, the pseudo-second-order model was not applicable to describe the adsorption process of Zr-cCNTs to catechol while the Double Constant equation can predict the kinetic process.

3.1.5. Effect of concentration and isotherm studies

The effects of the concentration of catechol on the adsorption process at three different temperatures are presented in Fig. 4d. It showed that the adsorption capacity increased with the augment of the equilibrium concentration, which may be due to the increase of the solution concentration provided a greater driving force for the adsorbate to overcome the mass transfer resistance between the aqueous phase and the solid phase [26]. In addition, as the initial concentration of the solution increased, the ratio of the number of adsorbate molecules to the available sites on the adsorbent surface increased, and the adsorption capacity enhanced accordingly. When the temperature increased from 293 to 313 K, the equilibrium adsorption capacity of Zr-cCNTs enhanced from 41.7 to 44.2 mg g⁻¹. The equilibrium adsorption capacity was enhanced with the increase of temperature, indicating that the adsorption of catechol by Zr-cCNTs was an endothermic process.

Langmuir, Freundlich and Koble–Corrigan isothermal adsorption models were used to fit the isotherms of adsorption of catechol by Zr-cCNTs.

$$q_e = \frac{q_m K_L C_e}{1 + K_L C_e} \quad (7)$$

$$q_e = K_F C_e^{1/n} \quad (8)$$

$$q_e = \frac{AC_e^n}{1 + BC_e^n} \quad (9)$$

where q_m are the maximum adsorption capacity while K_L is a constant related to the affinity of the binding sites and energy of adsorption (L mg⁻¹) whereas C_e is equilibrium concentration (mg L⁻¹); K_F relates to the adsorption capacity while $1/n$ relates to the adsorption intensity of Zr-cCNTs; A and B are Koble–Corrigan constants and C_e is equilibrium concentration (mg L⁻¹).

The fitted curves are shown in Fig. 4d, and the fitting parameters are shown in Table 2. It can be seen from Table 2, the adsorption capacity fitted by the Langmuir model was not significantly different from the experimental value. The value of R^2 was between 0.896 and 0.941, and SSE was comparatively high. Moreover, the fitted curves from the Langmuir model were not close to experimental points. These showed that the Langmuir model can predict

Table 2
Isotherm fitting parameters of adsorption for catechol by Zr-cCNTs

Langmuir					
T/K	$K_L/(L\text{ mg}^{-1})$	$q_{m(\text{exp})}/(\text{mg g}^{-1})$	$q_{m(\text{theo})}/(\text{mg g}^{-1})$	R^2	SSE
293	0.0534 ± 0.0112	41.7	43.5 ± 1.7	0.896	23.8
303	0.0594 ± 0.0112	42.7	44.5 ± 1.5	0.913	20.2
313	0.0726 ± 0.0109	44.2	45.2 ± 1.1	0.941	13.2
Freundlich					
T/K	K_F	$q_{m(\text{exp})}/(\text{mg g}^{-1})$	$1/n$	R^2	SSE
293	11.9 ± 1.1	41.7	0.273 ± 0.020	0.959	9.42
303	13.1 ± 1.1	42.7	0.226 ± 0.018	0.965	8.03
313	15.1 ± 1.0	44.2	0.204 ± 0.014	0.971	6.34
Koble–Corrigan					
T/K	A	B	n	R^2	SSE
293	10.9 ± 3.5	0.106 ± 0.109	0.350 ± 0.218	0.953	8.95
303	11.1 ± 3.6	0.143 ± 0.044	0.405 ± 0.182	0.965	6.73
313	11.5 ± 2.9	0.184 ± 0.022	0.479 ± 0.127	0.982	3.32

the adsorption capacity and is not proper to fit the whole curve. Comparing the R^2 and error values of these adsorption models, the R^2 of Freundlich and Koble–Corrigan models were all greater than 0.950 at three temperatures, and the SSE values were relatively small. The fitting parameter $1/n$ in the Freundlich model was between 0.2 and 0.3, indicating that Zr-cCNTs were easy to adsorb catechol [27]. With the increase of temperature, the K_F value enhanced from 11.9 to 15.1, which indicated that the adsorption process was an endothermic reaction. The fitting constant n of Koble–Corrigan model was less than 0.500, indicating that this model was more inclined to the Freundlich model. Of course, the fitted curves from Freundlich and Koble–Corrigan models were close to experimental points. So the adsorption process of catechol by Zr-cCNTs included multi-molecular layer adsorption, and the adsorbents had heterogeneity [28].

3.2. Thermodynamic parameters on the adsorption

The Gibbs free energy change (ΔG), enthalpy (ΔH) and entropy change (ΔS) were used to illustrate the adsorption process of spontaneity, the increase and decrease of energy and entropy. The calculation formulas of thermodynamic parameters are as follows:

$$K_c = \frac{C_{\text{ad},e}}{C_e} \quad (10)$$

$$\Delta G = -RT \ln K'_c \quad (11)$$

$$\Delta G = \Delta H - T\Delta S \quad (12)$$

where $C_{\text{ad},e}$ is the concentration of catechol on Zr-cCNTs at adsorption equilibrium, C_e is the concentration of catechol at equilibrium, R ($8.314\text{ J mol}^{-1}\text{ K}^{-1}$) is the ideal gas constant,

$T(\text{K})$ is the temperature of this reaction. K_c is the apparent adsorption constant.

It needs to be calculated in an ideal state of extremely dilute solution. Therefore, the lowest point or the first few points of equilibrium concentration in the adsorption isotherm were picked to calculate $\ln K_c$. Then plot C_e with $\ln K_c$. The vertical axis of linear and intersection is $\ln K'_c$. Substituting the value of K_c into Eq. (11) can obtain ΔG at three temperatures. Plot ΔG against T , the slope of the straight line is ΔS , and the intersection with the longitudinal axis is ΔH .

The apparent activation energy E_a (kJ mol^{-1}) can judge the difficulty of the adsorption reaction. The smaller the value, the easier the adsorption reaction is. It is generally believed that the E_a value between 5 and 40 kJ mol^{-1} is physical adsorption, while the E_a value higher than 40 kJ mol^{-1} is chemical adsorption. The expression is shown in Eq. (13).

$$\ln k = -\frac{E_a}{RT} + \ln A \quad (13)$$

where A is the temperature impact factor, k is the adsorption rate constant and $T(\text{K})$ is the reaction temperature.

According to Eqs. (10)–(13), the adsorption thermodynamic parameters of catechol by Zr-cCNTs were calculated, and the results were shown in Table 3.

The thermodynamic parameters showed that ΔG values were all less than zero, suggesting that the adsorption reaction of catechol by Zr-cCNTs can proceed spontaneously. With the increase of the reaction temperature from 293 to 313 K, the ΔG value decreased from 0.711 to 1.27 kJ mol^{-1} . It indicated that the increase of temperature enhanced the spontaneity of the adsorption reaction. The high temperature made the adsorption of catechol by Zr-cCNTs easier. A positive value of ΔH suggested that the adsorption process was an endothermic reaction. A positive value of ΔS demonstrated that the randomness of the adsorbent/

Table 3
Thermodynamic parameters for the adsorption of catechol by Zr-cCNTs

E_a /(kJ mol ⁻¹)	ΔH /(kJ mol ⁻¹)	ΔS /(J mol ⁻¹ K ⁻¹)	ΔG /(kJ mol ⁻¹)		
			293 K	303 K	313 K
22.5	7.45	27.8	-0.711	-0.949	-1.27

adsorbate interface increased during adsorption. It may be due to the change of adsorbent structure during the adsorption process [29]. The value of E_a was 22.5 kJ mol⁻¹, ranging from 5 to 40 kJ mol⁻¹, indicating that there was physical adsorption during the adsorption of catechol by Zr-cCNTs.

3.3. Reusability and stability studies

To test the reuse of the spent or exhausted adsorbent or recovery the adsorbate-loaded on the adsorbent, a desorption study can be performed and this makes the process economical and effective [30–33]. Four methods were used to desorb catechol adsorbed by Zr-cCNTs. Desorption rate d and regeneration rate r were calculated respectively under different conditions, as shown in Fig. 5a. The solution with better desorption and regeneration effect was selected to carry out multiple desorptions and regeneration studies on the adsorbent. The results are shown in Fig. 5b.

As can be seen from Fig. 5a, the desorption rate of Zr-cCNTs in the four desorption fluids was lower than 20% and the regeneration rate was below 60%. This showed that the adsorption of Zr-cCNTs was mainly complexation, and the acting force was strong. After desorption, there was a certain regeneration rate due to the increase of active sites. Fig. 5b shows the results of the desorption and regeneration

of Zr-cCNTs three times with 0.1 mol L⁻¹ HCl. The desorption rate and regeneration rate decreased with the increase of experimental times.

In this study, Zr loading and dissolution were determined by xylenol orange spectrophotometry. In the preparation process, the loading amount of zirconium was measured to be about 166 mg g⁻¹, Zr-cCNTs were shaken in distilled water for 12 h and then the content of zirconium in the solution was determined by centrifugal separation. The experimental results showed that the properties of Zr-cCNTs were stable and the zirconium dissolution was 0.114 mg g⁻¹. This also indicated that the low regeneration rate of Zr-cCNTs to catechol is not due to the dissolution of zirconium on the material.

3.4. Selective adsorption

In order to further verify the selective adsorption and mechanism of catechol by Zr-cCNTs, the adsorption constant k for single-component adsorption capacity of cMWCNTs and Zr-cCNTs to different adsorbates, catechol, *p*-chlorophenol (*p*-CP) and resorcinol, under the same reaction conditions was compared. The results are shown in Table 4. According to the table, the value of the equilibrium constant k (q_e/C_e) of catechol was significantly higher

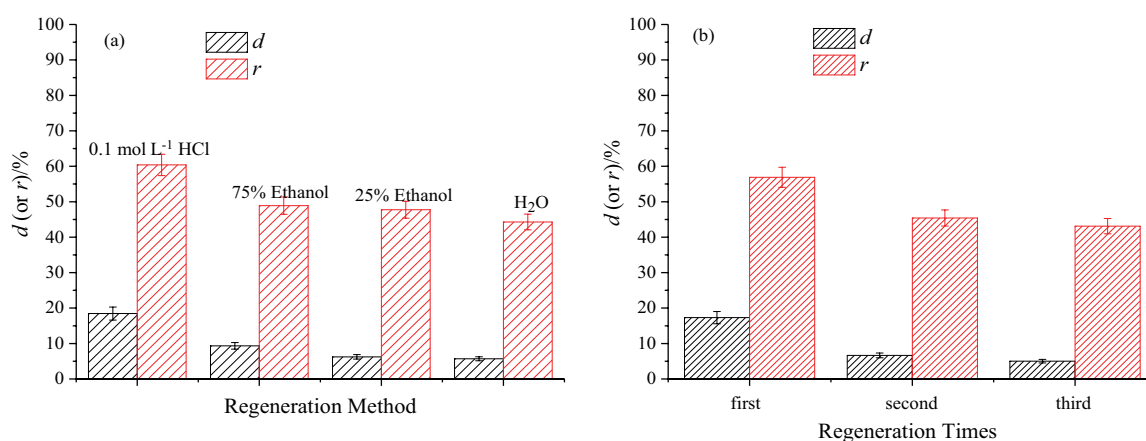


Fig. 5. Desorption and regeneration of catechol by Zr-cCNTs of different methods (a) and three times (b) with 0.1 mol L⁻¹ HCl.

Table 4
Adsorption constant and unit adsorption capacity of Zr-cCNTs for different adsorbates

C_0 (100 mg L ⁻¹)	Catechol		<i>p</i> -CP		Resorcinol	
	K	q_e /(mg g ⁻¹)	K	q_e /(mg g ⁻¹)	K	q_e /(mg g ⁻¹)
cMWCNTs	1.04	9.39	3.18	24.1	0.777	7.21
Zr-cCNTs	4.97	33.2	3.32	24.9	1.11	10.3

than that of *p*-CP and resorcinol. The adsorption capacity of Zr-cCNTs toward catechol was significantly higher than that of cMWCNTs in the same conditions. After that, competitive adsorption research was carried out. The mixed liquor of catechol/*p*-CP and catechol/resorcinol was adsorbed by Zr-cCNTs. Then the unit adsorption capacity of the adsorbent in the mixture was compared. The experimental results demonstrated that the adsorption capacity of Zr-cCNTs to catechol and *p*-CP in the mixed solution was 23.6 and 20.1 mg g⁻¹, respectively. In the mixture of catechol/resorcinol, the adsorption capacity of Zr-cCNTs to catechol and resorcinol was 19.7 and 8.56 mg g⁻¹, respectively.

In summary, the adsorption capacity of Zr-cCNTs toward catechol was higher than that of other adsorbents in both single-component and two-component systems, which also proved the selective adsorption of Zr-cCNTs to catechol as it is o-dihydroxy in the structure of catechol.

3.5. XPS analysis and adsorption mechanism

The adsorption mechanism of catechol by Zr-cCNTs was analyzed by XPS. Fig. 6 shows the full XPS spectrum before and after the adsorption. As can be seen from Fig. 6, the full XPS spectra before and after the adsorption showed little change, in which the percentage of C1s and the peak strength enhanced. The high-resolution XPS

spectral analysis of Zr3d and O1s in Zr-cCNTs before and after adsorption is shown in Fig. 6.

This suggested that that catechol successfully adsorbed on the surface of Zr-cCNTs. It can be seen that after adsorption

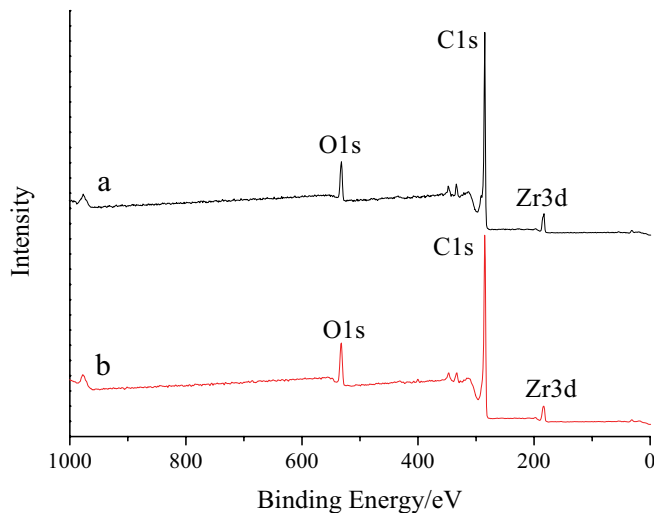


Fig. 6. Comparison of XPS spectra before (a) and after (b) the adsorption.

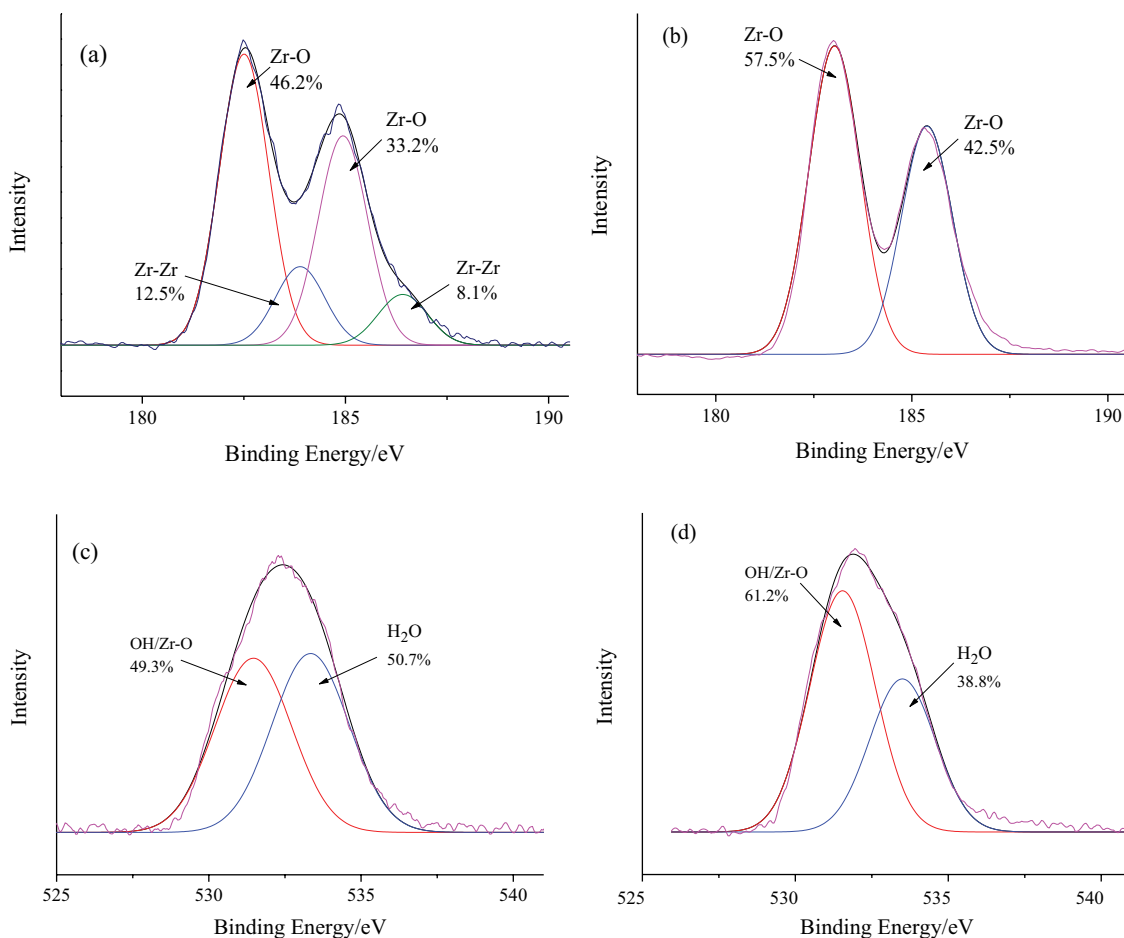


Fig. 7. Peak separation of Zr3d before (a) and after (b) adsorption; O1s before (c) and after (d) adsorption.

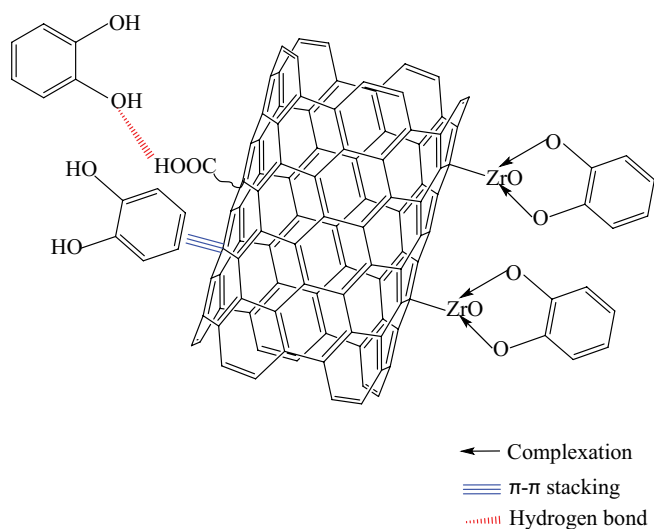


Fig. 8. Complexation mechanism diagram of Zr-cCNTs and catechol.

of catechol, Zr3d is divided into two peaks, 183.02 and 185.38 eV, corresponding to the Zr–O bond. The percentage enhanced to 57.5% and 42.5%. The binding energy of OH/Zr–O increased from 531.46 to 531.54 eV after adsorption of catechol. The percentage enhanced from 49.3% to 61.2%. XPS analysis illustrated that the adsorption of catechol by Zr-cCNTs may be due to the combination of zirconium on the adsorbent surface and OH in catechol to form Zr–O bond. Combined with zirconium adsorption properties and the structural formula of catechol, it can be seen that the Zr loaded on the surface of cMWCNTs may be complexed with catechol to form a stable five-member ring. Fig. 8 shows the complexation process of zirconium and o-dihydroxyl on the adsorbent surface. The main force of Zr-cCNTs toward catechol was complexation. However, the adsorption of catechol by carbon nanotubes without Zr modification is related to hydrogen bonding force and π – π stacking.

4. Conclusion

The adsorption capacity of cCNTs toward catechol was enhanced after Zr modification. The adsorption of catechol on Zr-cCNTs was reached equilibrium in 60 min and basically unaffected by pH and the coexistence of Cl^- and SO_4^{2-} in solution. The inner layer complexation plays a major role in the adsorption process. There is heterogeneous surface multi-molecular layer adsorption. The thermodynamic study showed that the adsorption of catechol by Zr-cCNTs was a spontaneous, endothermic and entropy-increasing physical and chemical adsorption process. Zr-cCNTs has a strong binding force to catechol and it is promising to remove catechol from solution.

Acknowledgements

This work was financially supported by the Henan province basis and advancing technology research project in China (142300410224).

References

- [1] J.H. Kim, S.-G. Hong, H.J. Sun, S. Ha, J.B. Kim, Precipitated and chemically-crosslinked laccase over polyaniline nanofiber for high performance phenol sensing, *Chemosphere*, 143 (2016) 142–147.
- [2] Q. Liao, J. Sun, L. Gao, The adsorption of resorcinol from water using multi-walled carbon nanotubes, *Colloids Surf., A*, 312 (2008) 160–165.
- [3] R. Sridar, U. Uma Ramanane, M. Rajasimman, ZnO nanoparticles – synthesis, characterization and its application for phenol removal from synthetic and pharmaceutical industry wastewater, *Environ. Nanotechnol. Monit. Manage.*, 10 (2018) 388–393.
- [4] Y.H. Fu, Y.F. Shen, Z.D. Zhang, X.L. Ge, M.D. Chen, Activated bio-chars derived from rice husk via one- and two-step KOH-catalyzed pyrolysis for phenol adsorption, *Sci. Total Environ.*, 646 (2019) 1567–1577.
- [5] N.N. Dutta, S. Borthakur, R. Baruah, A novel process for recovery of phenol from alkaline wastewater laboratory study and predesign cost estimate, *Water Environ. Res.*, 70 (1998) 4–9.
- [6] B.X. Xie, J.H. Qin, S. Wang, H. Sun, W.Q. Chen, Adsorption of phenol on commercial activated carbons: modelling and interpretation, *Int. J. Environ. Res. Public Health*, 17 (2020) 789, doi: 10.3390/ijerph17030789.
- [7] Y. Wang, L.H. Yang, X. Chen, X. Zhang, G.C. Li, X.B. Li, S. Chen, Aldol condensation followed by ozonation to reduce phenolic compounds in coking wastewater, *IOP Conf. Ser.: Earth Environ. Sci.*, 510 (2020) 042031.
- [8] G. Crini, E. Lichtfouse, L.D. Wilson, N. Morin-Crini, Conventional and non-conventional adsorbents for wastewater treatment, *Environ. Chem. Lett.*, 17 (2019) 195–1213.
- [9] A. Mohammadi, P. Veisi, High adsorption performance of β -cyclodextrin-functionalized multi-walled carbon nanotubes for the removal of organic dyes from water and industrial wastewater, *J. Environ. Chem. Eng.*, 6 (2018) 4634–4643.
- [10] Z.Y. Ruan, Y.X. Tian, J.F. Ruan, G.J. Cui, K. Iqbal, A. Iqbal, H.R. Ye, Z.Z. Yang, S.Q. Yan, Synthesis of hydroxyapatite/multi-walled carbon nanotubes for the removal of fluoride ions from solution, *Appl. Surf. Sci.*, 412 (2017) 578–590.
- [11] R. Kamaraj, S. Vasudevan, Decontamination of selenate from aqueous solution by oxidized multi-walled carbon nanotubes, *Powder Technol.*, 274 (2015) 268–275.
- [12] M.Y. Liu, X.T. Zhang, Z.H. Li, L.B. Qu, R.P. Han, Fabrication of zirconium(IV)-loaded chitosan/ Fe_3O_4 /graphene oxide for efficient removal of alizarin red from aqueous solution, *Carbohydr. Polym.*, 248 (2020) 116792, doi: 10.1016/j.carbpol.2020.116792.
- [13] L.J. Huang, M. He, B.B. Chen, B. Hu, Magnetic Zr-MOFs nanocomposites for rapid removal of heavy metal ions and dyes from water, *Chemosphere*, 199 (2018) 435–444.
- [14] C.H. Ma, X.T. Zhang, K. Wen, R. Wang, R.P. Han, Facile synthesis of polyethyleneimine/ Fe_3O_4 loaded with zirconium for enhanced phosphate adsorption: performance and adsorption mechanism, *Korean J. Chem. Eng.*, 38 (2021) 135–143.
- [15] J.H. Huang, K.L. Huang, C. Yan, Application of an easily water-compatible hypercrosslinked polymeric adsorbent for efficient removal of catechol and resorcinol in aqueous solution, *J. Hazard. Mater.*, 167 (2009) 69–74.
- [16] R.L. Xu, Y. Peng, Preparation of magnetic g- C_3N_4 / Fe_3O_4 composite and its application in the separation of catechol from water, *Materials*, 12 (2019) 2844, doi: 10.3390/ma12182844.
- [17] Y.F. Gu, M.M. Yang, W.L. Wang, R.P. Han, Phosphate adsorption from solution by zirconium loaded carbon nanotubes in batch mode, *J. Chem. Eng. Data*, 64 (2019) 2849–2858.
- [18] A. Mullick, S. Neogi, Acoustic cavitation induced synthesis of zirconium impregnated activated carbon for effective fluoride scavenging from water by adsorption, *Ultrason. Sonochem.*, 45 (2018) 65–77.
- [19] L.H. Velazquez-Jimenez, R.H. Hurt, J. Matos, J.R. Rangel-Mendez, Zirconium-carbon hybrid sorbent for removal of fluoride from water: oxalic acid mediated Zr(IV) assembly

- and adsorption mechanism, *Environ. Sci. Technol.*, 48 (2014) 1166–1174.
- [20] D.C. Liu, S.B. Deng, A. Maimaiti, B. Wang, J. Huang, Y.J. Wang, G. Yu, As(III) and As(V) adsorption on nanocomposite of hydrated zirconium oxide coated carbon nanotube, *J. Colloid Interface Sci.*, 511 (2018) 277–284.
- [21] W.H. Xu, J. Wang, L. Wang, G.P. Sheng, J.H. Liu, H.Q. Yu, X.J. Huang, Enhanced arsenic removal from water by hierarchically porous CeO₂-ZrO₂ nanospheres: role of surface- and structure-dependent properties, *J. Hazard. Mater.*, 260 (2013) 498–507.
- [22] H. Gulley-Stahl, P.A. Hogan, W.L. Schmidt, S.J. Wall, A. Bührlage, H.A. Bullen, Surface complexation of catechol to metal oxides: an ATR-FTIR, adsorption, and dissolution study, *Environ. Sci. Technol.*, 44 (2010) 4116–4121.
- [23] A.A. Aryee, F.M. Mpatani, X.T. Zhang, A.N. Kani, E. Dovi, R.P. Han, Z.H. Li, L.B. Qu, Iron(III) and iminodiacetic acid functionalized magnetic peanut husk for the removal of phosphate from solution: characterization, kinetic and equilibrium studies, *J. Cleaner Prod.*, 268 (2020) 122191, doi: 10.1016/j.jclepro.2020.122191.
- [24] M.B. McBride, A critique of diffuse double layer models applied to colloid and surface chemistry, *Clays Clay Miner.*, 45 (1997) 598–608.
- [25] Y.Y. Hu, R.P. Han, Selective and efficient removal of anionic dyes from solution by zirconium (IV) hydroxide coated magnetic materials, *J. Chem. Eng. Data.*, 64 (2019) 791–799.
- [26] A.A. Aryee, E. Dovi, R.P. Han, Z.H. Li, L.B. Qu, One novel composite based on functionalized magnetic peanut husk as adsorbent for efficient sequestration of phosphate and Congo red from solution: characterization, equilibrium, kinetic and mechanism studies, *J. Colloid Interface Sci.*, 598 (2021) 69–82.
- [27] R. Kamaraj, A. Pandiarajan, M. Rajiv Gandhi, A. Shibayama, S. Vasudevan, Eco-friendly and easily prepared graphene nanosheets for safe drinking water: removal of chlorophenoxyacetic acid herbicides, *Chem. Select.*, 2 (2017) 342–355.
- [28] H.T. Li, Y.C. Jiao; M.C. Xu, Z.Q. Shi, B.Q. He, Thermodynamics aspect of tannin sorption on polymeric adsorbents, *Polymer*, 45 (2004) 181–188.
- [29] M. Kapnisti, F. Noli, P. Misaelides, G. Vourlias, D. Karfaridis, A. Hatzidimitriou, Enhanced sorption capacities for lead and uranium using titanium phosphates; sorption, kinetics, equilibrium studies and mechanism implication, *Chem. Eng. J.*, 342 (2018) 184–195.
- [30] A.A. Aryee, E. Dovi, X.X. Shi, R.P. Han, Z.H. Li, L.B. Qu, Zirconium and iminodiacetic acid modified magnetic peanut husk as a novel adsorbent for the sequestration of phosphates from solution: characterization, equilibrium and kinetic study, *Colloids Surf., A*, 615 (2021) 126260, doi: 10.1016/j.colsurfa.2021.126260.
- [31] H.N. Bhatti, Z. Mahmood, A. Kausar, S.M. Yakout, O.H. Shair, M. Iqbal, Biocomposites of polypyrrole, polyaniline and sodium alginate with cellulosic biomass: adsorption-desorption, kinetics and thermodynamic studies for the removal of 2,4-dichlorophenol, *Int. J. Biol. Macromol.*, 153 (2020) 146–157.
- [32] A.A. Aryee, F.M. Mpatani, A.N. Kani, E. Dovi, R.P. Han, Z.H. Li, L.B. Qu, A review on functionalized adsorbents based on peanut husk for the sequestration of pollutants in wastewater: modification methods and adsorption study, *J. Cleaner Prod.*, 310 (2021) 127502, doi: 10.1016/j.jclepro.2021.127502.
- [33] B.L. Zhao, W. Xiao, Y. Shang, H.M. Zhu, R.P. Han, Adsorption of light green anionic dye using cationic surfactant-modified peanut husk in batch mode, *Arabian J. Chem.*, 10 (2017) S3595–S3602.